Article

Chinese Science Bulletin

Progress of Projects Supported by NSFC
Oceanology

October 2012 Vol.57 No.28-29: 3748–3760
doi: 10.1007/s11434-012-5277-x

Late Quaternary glacial cycle and precessional period of clay mineral assemblages in the Western Pacific Warm Pool

WU JiaWang, LIU ZhiFei* & ZHOU Chao

State Key Laboratory of Marine Geology, Tongji University, Shanghai 200092, China

Received December 30, 2011; accepted April 18, 2012; published online July 26, 2012

Variability of clay mineral assemblages in the Western Pacific Warm Pool (WPWP) over the past 370 ka shows the prominent glacial-interglacial cyclicity. Smectite (62%–91%) is the dominant clay mineral, with decreased contents during interglacials while increased in glacials. In contrast, variations in chlorite (4%–21%), illite (4%–12%), and kaolinite (2%–10%) share a similar pattern with higher contents during interglacials than glacials, mirroring to that of smectite. The results indicate that the smectite-dominated clay minerals derive mainly from the river detrital inputs of New Guinea. The glacial-interglacial cycle of clay mineral assemblages well correspond to the fluctuation of sea level. When the sea level was low, the river materials can travel more easily across the narrow shelf off the island of New Guinea, inject directly into the subsurface currents flowing westwards, then merge into the Equatorial Undercurrent (EUC), and eventually deposit on the central part of WPWP. Precessional periods of the smectite content indicate the intensity of mechanical erosion in its provenance of New Guinea, responding to the river runoff and precipitation, and this could also be linked to the meridional migration of the Intertropical Convergence Zone (ITCZ).

clay minerals, glacial cycle, precessional period, Intertropical Convergence Zone (ITCZ), late Quaternary, Western Pacific Warm Pool (WPWP)

Citation: Wu J W, Liu Z F, Zhou C. Late Quaternary glacial cycle and precessional period of clay mineral assemblages in the Western Pacific Warm Pool. Chin Sci Bull, 2012, 57: 3748–3760, doi: 10.1007/s11434-012-5277-x

The Western Pacific Warm Pool (WPWP) is a region with the maximal solar radiation, the highest Sea Surface Temperature (SST), and the most active monsoon circulation, and therefore the largest seasonal migration magnitude of the Intertropical Convergence Zone (ITCZ) [1]. Consequently, accompanied by the large-scale overturning of atmospheric circulation and the extensive shift of precipitation zone, the meridional displacement of the ITCZ dominates the seasonal climatic and environmental changes in SST, Sea Surface Salinity (SSS), precipitation, land runoff, and land vegetation over the region of WPWP [2–4].

The region of WPWP is dominated by abundant rainfall and warm climate conditions throughout the year, making it the strongest weathering and denudation area in the world. Along with continents and islands in South and East Asia, the annual terrigenous sediment discharge to the ocean accounts for around 70% of the total world input [5]. In particular, even though the island of New Guinea covers 8×10^5 km^2 area only, its fluvial discharge is approximate 1.7×10^9 t a^{-1}, in proportion to the value resulting from the entire North America [6,7].

Such active precipitation zone and abundant terrigenous input make the WPWP a significant scientific position to study the land-sea interactions. Previous studies in the WPWP paid attentions to the SST and SSS characters [8,9], or emphasized the importance of Source-to-Sink (S2S) modern process of fluvial sediment input [10,11]. However, the temporal variation in terrigenous material sedimentation in the WPWP is poorly known. As clay minerals are the most important terrigenous detrital fractions in marine sediments, the temporal variation in clay mineral assemblages not only reveals the contemporaneous weathering and erosion occurred in continental source areas [12,13], but also deciphers controlling characters of provenance supply and

*Corresponding author (email: lzhifei@tongji.edu.cn)

current transport [14,15].

In this study, we select Core KX21-2 and several core-top samples, which were collected from the central part of WPWP during the Western Pacific Cruise (KX08-973) of the "Ocean Carbon Cycle and Tropical Forcing of Climate Evolution (a National Basic Research Program of China)" onboard R/V Kexue-1 in December 2008. Temporal variations in clay mineral assemblages and provenance analysis, combined with X-ray Fluorescence (XRF) core scanning data, are analyzed to study weathering and erosion processes and their responses to glacial cycle and precessional period over the last 370 ka of late Quaternary in the region of WPWP.

1 Regional background

Core KX21-2 is located on the Ontong Java Plateau in the central part of WPWP, which is delineated by the 29°C isotherm in the SST (Figure 1). Previous studies suggested that the island of New Guinea, lying to the southwest of Core KX21-2, is an important provenance of terrigenous materials for the Ontong Java Plateau [10,16–18].

New Guinea is under the control of equatorial air mass throughout the year, forming high temperature and heavy rainfall climate conditions. Owing to the shift of ITCZ, the influence of monsoon circulation, and the high mountain relief, the distribution of precipitation zone varies seasonally and is differentiated among various areas. The annual rainfall is about 2500–3000 mm in the northern coastal area, and as high as 4000 mm in the central mountain area (http://www.worldweather.org). From November to April, the northwest monsoon prevails when the ITCZ shifts southwards, causing the major rain season in New Guinea; while during May through October, the southeast monsoon prevails when the ITCZ moves northwards, resulting in the reduced precipitation [18–20].

Northwest-southeast extending mountain ranges with elevations of generally higher than 4000 m compose the central part of New Guinea, where most rivers originated. Numerous islands generated from volcanism or coral reefs are distributed in the coastal region. The lithology of New Guinea consists mainly of intermediate-basic volcanic rocks and Quaternary sedimentary rocks, accompanied by intermediate-basic intrusive rocks and metamorphic rocks (Figure 1) [21]. Due to the impact of high mountain relief on the atmosphere circulation, the central mountain area suffers from extremely strong rainfall (12000 mm a^{-1}) [11,22]. Along with tectonic activities including earthquake and volcanic eruption, relatively young rocks in New Guinea are easily eroded, resulting in frequent mountainous torrents, debris flows, and other transport processes [5,6]. Hence, although the water discharge of New Guinea is relatively small, only accounting for 70% of the Amazon's, its sediment delivery value is about 1.5 times [6,7].

New Guinea provides fluvial sediments as high as 1.7×10^9 t a^{-1}, however, within which how many could be transported into the deep sea depends on various sedimentary environments, including shelf gradient, transport pathways, current patterns, etc. [11]. In the southern New Guinea, the Gulf of Papua (GOP) has a broad (~150 km) and gentle (gradient ~1:750) shelf (Figure 1) [11]. Previous studies suggested that the majority of river sediment load with sources mainly from the Fly River accumulates at their estuaries, instead of crossing the shelf, and only a very small part (<5%, [11]) could be carried into the deep sea by means of nepheloid layers [10,23,24]. The northern New Guinea is situated at the leading edge of the Australian Plate and yields fluvial sediments as high as 0.86×10^9 t a^{-1}, but the transport of sediments behaves very differently [6,7]. Taking the Sepik River for example (Figure 1), the shelf is very narrow (<10 km) and steep (gradient ~1:50), and a submarine canyon is extended to its estuary [11]. Considering the very limited accommodation space on the shelf, the filled trench, and the underestimate of abrupt events (e.g. debris flow) [7], ~90% of fluvial materials could be transported bypassing the continental shelf along submarine canyons and then into the deep sea [10].

The geographical distribution of New Guinea and its adjacent archipelago along with effect of the South Equatorial Current (SEC) make up a complicated oceanic circulation configuration (Figure 1) [25–29]. Surface currents are controlled by the monsoon system, flowing southeastwards from November to April and northwestwards from May to October, e.g. the New Guinea Coastal Current (NGCC) [28]. Subsurface currents (water depth ranging from 50 to 400 m) are relatively stable and affected less by winds and tides. Suffering from the barrier function of lands and islands, the SEC is separated into several subsurface current systems, including the Great Barrier Reef Undercurrent (GBRUC), the New Guinea Coastal Undercurrent (NGCUC), the St. Georges Undercurrent (SGUC), and the New Ireland Coastal Undercurrent (NICUC), all eventually merging into the Equatorial Undercurrent (EUC) (Figure 1).

2 Materials and methods

Core KX21-2 (1°25.01′S, 157°58.91′E, 1897 m water depth, original number KX08-97321-2) is 6.31 m long and consists mainly of gray foraminifera-rich ooze without apparent bioturbation. The age model, established by the planktonic foraminifer (*Globegerinoides ruber*) oxygen isotope stratigraphy (δ^{18}O) through correlating with the standard LR04 Stack, indicates that the bottom of Core KX21-2 is at the marine isotope stage (MIS) 10 with an approximate age of 370 ka BP [30]. A total of 425 samples with an average temporal resolution of 0.8 ka were sampled from Core KX21-2 for the clay mineralogy analysis. The procedure is to sample the core at a thickness interval of 5 cm firstly and

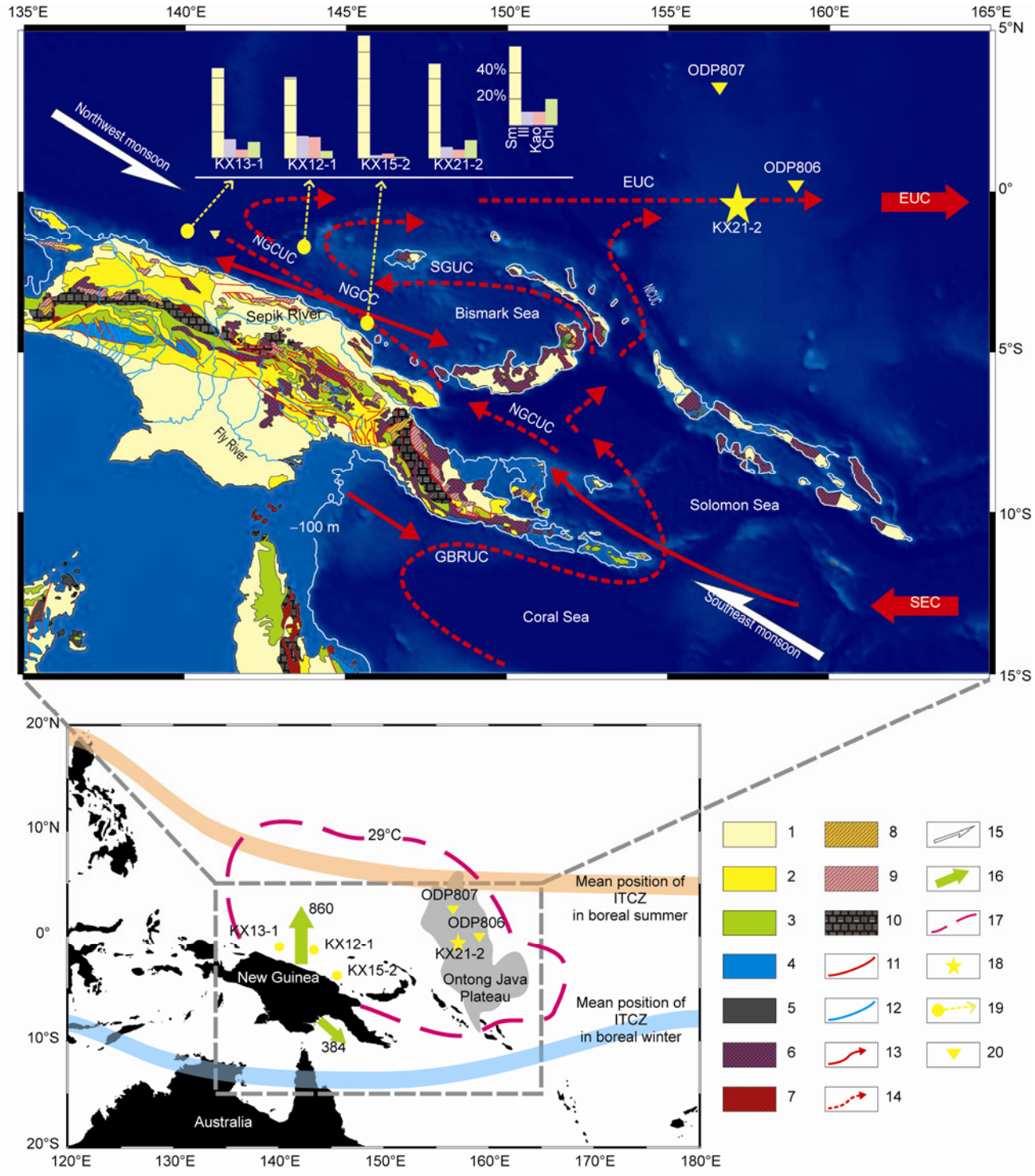

Figure 1 Regional geology and oceanography map of the Western Pacific Warm Pool (WPWP), showing the location of studied core. 1, Quaternary sediments; 2, Tertiary sedimentary rocks; 3, Mesozoic sedimentary rocks; 4, Paleozoic sedimentary rocks; 5, Precambrian sedimentary rocks; 6, intermediate-basic extrusive rocks; 7, acid intrusive rocks; 8, intermediate intrusive rocks; 9, basic intrusive rocks; 10, metamorphic rocks; 11, faults; 12, rivers; 13, surface currents [28]: New Guinea Coastal Current (NGCC); 14, subsurface current systems [23–29]: South Equatorial Current (SEC), Great Barrier Reef Undercurrent (GBRUC), New Guinea Coastal Undercurrent (NGCUC), St. Georges Undercurrent (SGUC), New Ireland Coastal Undercurrent (NICUC) and Equatorial Under Current (EUC); 15, monsoon systems [11,18]; 16, fluvial sediment inputs (10^6 t a^{-1}) [6,7]; 17, the central WPWP; 18, site of this study: Core KX21-2; 19, locations and clay mineral assemblages of three core-top samples; 20, other sites mentioned in this study. Regional geology map modified after [21]. Mean positions of the ITCZ after [1].

then further to sample at 1 cm interval at each deglacial period. Three core-top samples collected off the northern coast of New Guinea were also measured for the clay mineral assemblages. High-resolution elemental geochemistry (XRF core scanning) was analyzed on Core KX21-2. In addition, the photomicrography of clay minerals was conducted on a few randomly selected samples.

Clay minerals were identified by X-ray diffraction (XRD) on oriented mounts of clay-sized particles (<2 μm) [31]. Sample pretreatment and oriented mounts preparation followed the methodology of refs. [15,32]. The analysis was conducted using a PANalytical X'Pert PRO diffractometer with CuKα radiation and Ni filter, under a voltage of 45 kV and an intensity of 40 mA. Three XRD analysis runs were performed, following air-drying, ethylene-glycol solvation for 24 h, and heating at 490°C for 2 h.

Identification and interpretation of clay minerals were made according to a comprehensive comparison of three multiple X-ray diffratograms obtained under different measurement conditions [15,32]. Semi-quantitative calculations of each peak's parameters were carried out on the glycolated curve by using the MacDiff software [33]. The relative contents of each clay mineral species were estimated mainly according to area of (001) series of basal reflections, i.e. smectites (001) including illite/smectite random mixed-layers at 1.7 nm, illite (001) at 1 nm, and kaolinite (001) and chlorite (002) at 0.7 nm. Kaolinite and chlorite were discriminated according to the relative proportions given by a ratio of the 0.357 nm and 0.354 nm peak areas. Based upon the XRD method, the semi-quantitative evaluation of each clay mineral has an accuracy of 5% [31]. Replicate analyses of a few selected samples gave a precision of ±2% (2σ) [34]. Additionally, smectite crystallinity was obtained from the half height width of the 1.7 nm peak on the glycolated curve. The higher values represent the lower crystallinity, which can be an indication of the stronger hydrolysis in tropical regions [35,36]. Besides, the feldspar/quartz ratio refers to the peak area of plagioclase and K-feldspar (0.319–0.324 nm) divided by that of quartz (0.426 nm), representing the content ratio of feldspar/quartz within the clay-sized fractions. The ratio indicates the intensity of erosion versus chemical weathering. This parameter has been confirmed by several successful applications [37,38].

The element geochemical analysis was performed on an Avaatech X-ray fluorescence (XRF) core scanner at 1 cm thickness interval. Element intensity was reported in counts per second (cps). In order to reduce the effects of dilution and variations in physical properties (e.g. density and water content), we adopted the total counts of elements measured under same voltage as a normalizing parameter to assess relative degrees of enrichment/depletion of a given element. In this study, the normalized iron intensity referred as "Fe" is employed to represent the iron content. The reliability of this proxy has been verified by Revel et al. [39], who used it to reflect the African monsoon evolution.

The surface morphology was conducted using a Phillips XL-30 Scanning Electron Microscope (SEM). An affiliated EDAX SDD Energy Dispersive Spectrometer (EDS) system was adopted to detect major element contents of the single mineral grain.

All preparations, measurements, and analyses of the above experiments were performed at the State Key Laboratory of Marine Geology, Tongji University. The Redfit 35 software Schulz and Mudelsee [40] developed was employed to run the spectral analysis.

3 Results

The clay mineralogy over the past 370 ka of late Quaternary at Core KX21-2 shows the strong glacial-interglacial cyclicity (Figure 2). Smectite (62%–91%) accounts for the overwhelming majority, with decreased contents during interglacials while increased during glacials, especially peaking at periods of the rapid sea level rise (i.e. deglacials). In contrast, chlorite (4%–21%), illite (4%–12%), and kaolinite (2%–10%) share a similar variation pattern with lower contents in glacials than interglacials, mirroring to that of smectite. Moreover, variations in the smectite content are well correlated positively to those in the feldspar/quartz ratio, and are broadly correlated inversely to those in the smectite crystallinity (Figure 3).

The clay mineral assemblages of three core-top samples collected off the northern coast of New Guinea are generally similar to those at Core KX21-2, consisting of dominant smectite and minor chlorite, illite, and kaolinite (Table 1). The samples closer to the coastline show the higher smectite contents (Figure 1). Core KX15-2 is located both in the Sepik River estuary and on the pathway of the NGCUC, and its smectite content reaches as high as 92%. The smectite crystallinity and feldspar/quartz ratio of this core-top

Table 1 Clay mineral assemblages and mineralogical parameters of core-top samples of Core KX21-2 and other three cores collected off the northern coast of New Guinea

Site	Latitude (S)	Longitude (E)	Smectite (%)	Illite (%)	Kaolinite (%)	Chlorite (%)	Smectite crystallinity (°Δ2θ)	Feldspar/quartz
KX21-2	01°25.01'	157°58.91'	71	9	7	14	0.79	6.50
KX12-1	01°48.82'	143°40.09'	61	17	16	6	0.99	6.34
KX13-1	01°14.36'	140°00.92'	68	14	6	12	0.91	8.48
KX15-2	04°07.26'	145°36.21'	92	3	4	1	0.76	11.96

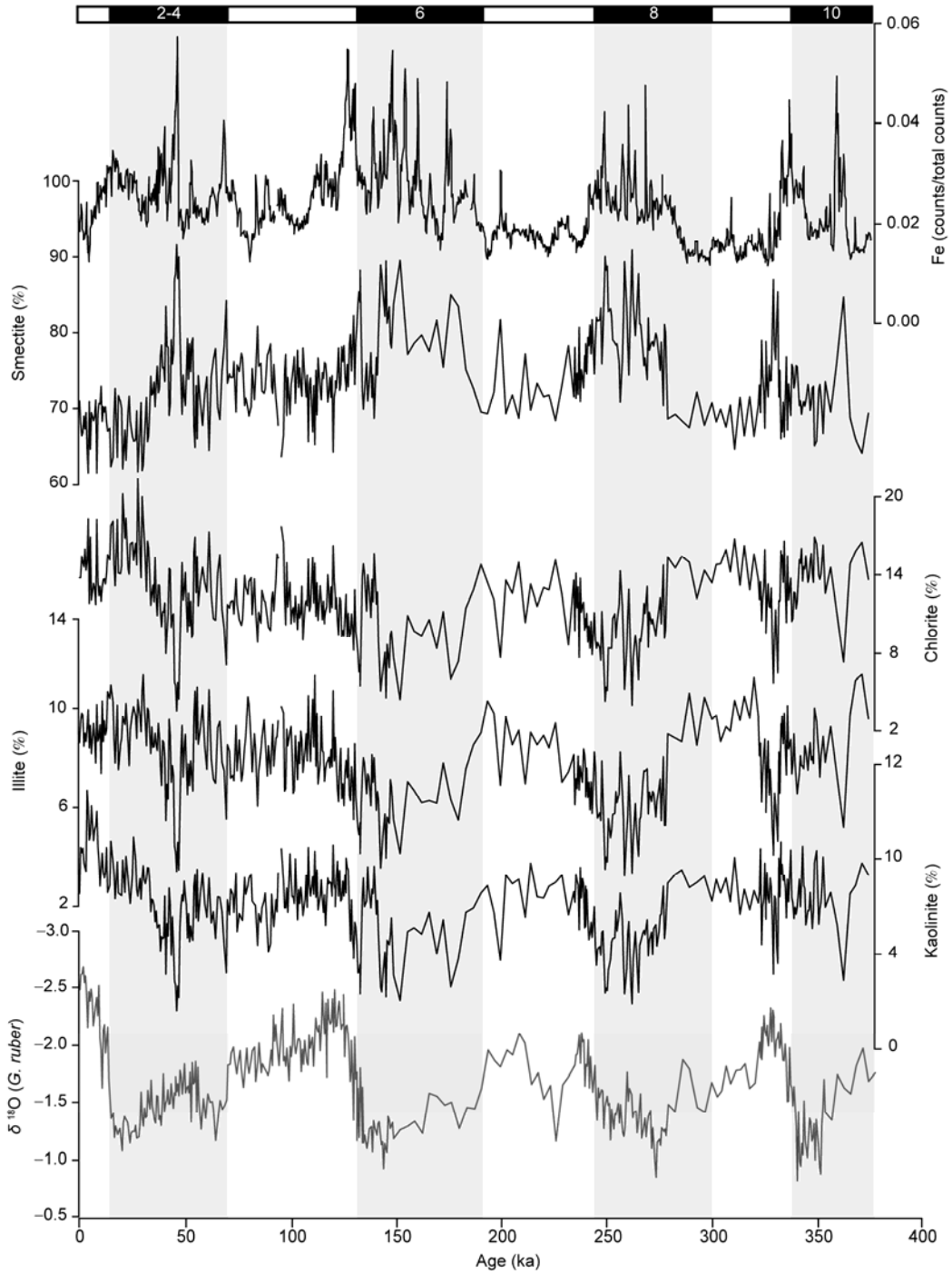

Figure 2 Clay mineral assemblages, Fe contents, and planktonic foraminifer oxygen isotope stratigraphy over the past 370 ka at Core KX21-2. The planktonic foraminifer oxygen isotope stratigraphy is after [30].

sample are much higher than those of other core-top samples (Table 1).

The semi-quantitative XRF geochemical analysis shows that variations in the Fe content not only consist with the smectite content but also present a higher frequency oscillation (Figure 2). The photomicrography of randomly selected samples indicates that clay mineral particles are mainly terrigenous without authigenic features (Figure 4).

4 Discussions

4.1 Formation of smectite

The formation of clay minerals in marine sediments is continuously being debated, generally depending on mineralogical characteristics, climatic and environmental conditions, and geological settings. Biscaye [41] established the

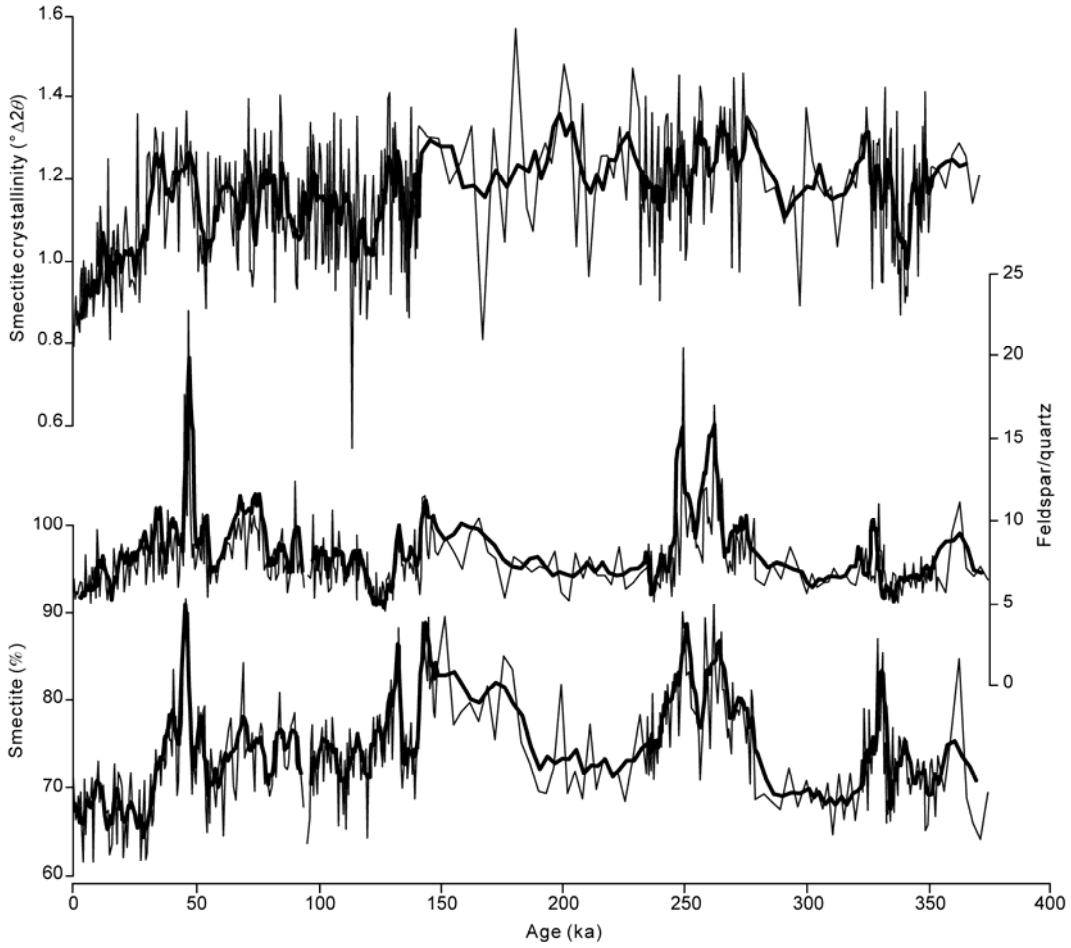

Figure 3 Correlations of smectite content, feldspar/quartz ratio, and smectite crystallinity at Core KX21-2. Bold lines are their five-point moving average, respectively.

semi-quantitative method using XRD. Thereafter, a large number of investigations showed the latitudinal zonations of the clay mineral distribution in world oceans, relating to the climate and lithology on adjacent land masses, and it is deduced that clay minerals in oceans derive mainly from continents, especially from soils [42,43]. For instance, the intensive weathering in tropical regions presents the growth of kaolinite; the prevalence of illite and chlorite in high latitudes reflects the denudation of glaciers. The K/Ar isotopic dating of illite in recent marine sediments in the North Atlantic showed the ages at an order of 10^8 years, indicating its adjacent old continental rocks and their weathered products sources [41]. Given some specific environments (e.g. pH conditions and elemental compositions), kaolinite and chlorite are difficult to be formed authigenicly in the ocean [43]. Although alteration of oceanic crust or contact metamorphism of marine sediments (intruded by basaltic lava) may generate the authigenic chlorite [12], the influence could be negligible because of its obvious characteristics and limited occurrence. Therefore, the content of the authigenic clay minerals in the ocean was estimated less than 10% [43].

However, the distribution of smectite abundance in recent marine sediments does not show a clear latitudinal pattern, but presents some regional increase. Three explanations could be considered: terrigenous input, differential settling, and authigenesis of smectite. Clay mineralogical analysis on surface sediment samples in rivers of Luzon by Liu et al. [36] demonstrated that the overwhelming majority of smectite (86%) results from the weathering of intermediate-basic volcanic rocks and becomes the principal source for smectite deposited in the northern South China Sea. The differential settling between smectite and kaolinite is usually used to interpret the distribution pattern of smectite. Relatively coarse kaolinite grains tend to settle down when running into the alkaline seawater, while fine smectite grains could be transported for a long distance following the oceanic current, causing its seaward enrichment. This phenomenon is best illustrated with typical examples of the northern Gulf of Mexico (the Mississippi River) [44] and the Gulf of Guinea (the Niger River) [45]. Considering some environmental conditions, such as low sedimentation rate, strong volcanic-hydrothermal activity, and development of metalliferous sedimentary deposit, the enrichment

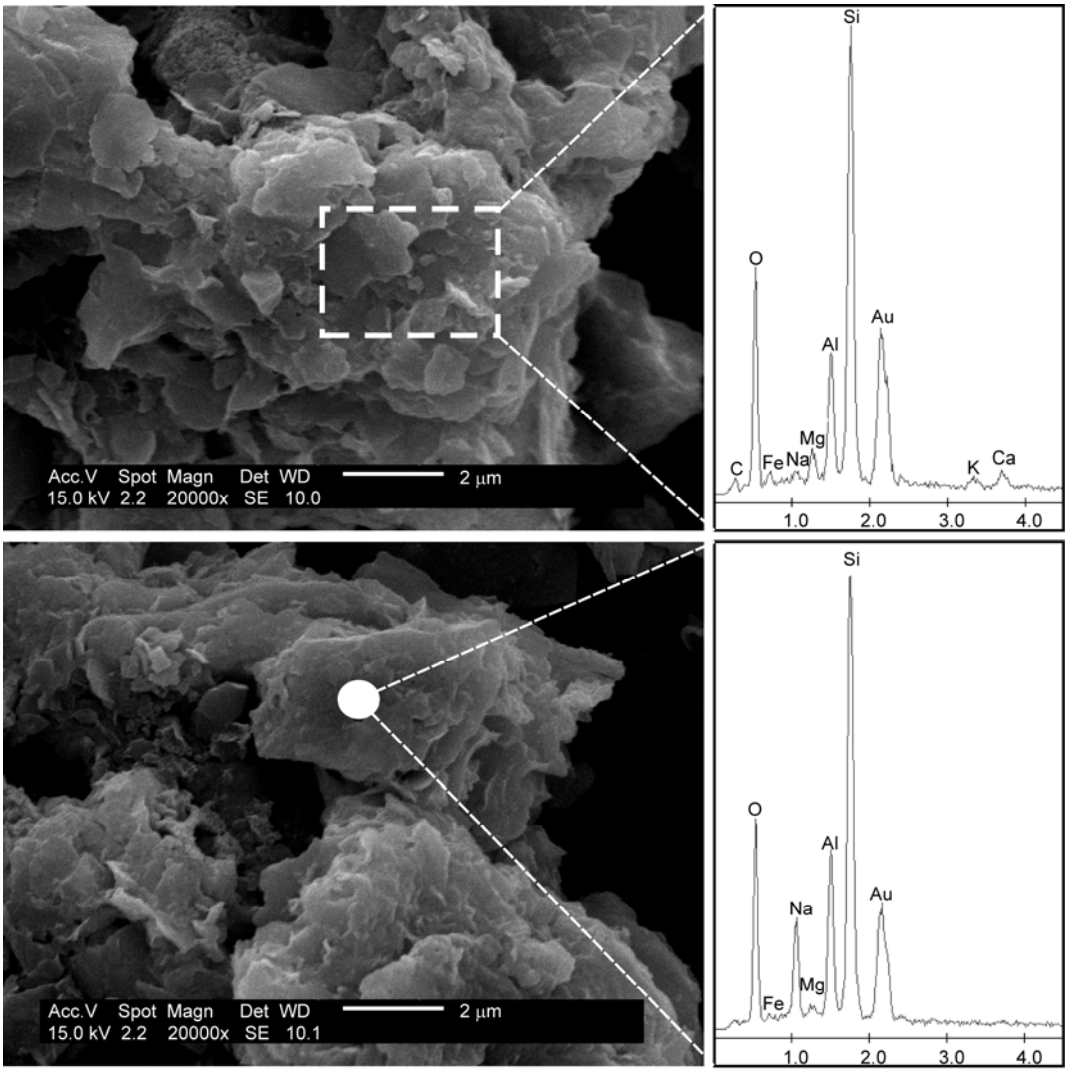

Figure 4 SEM photos (left) of randomly selected samples (<20 μm) at Core KX21-2 and their affiliated EDS spectra (right). The samples are located at a depth of 0.85 m (upper) and 5.30 m (lower) of Core KX21-2.

of smectite in South Pacific is generally regarded as authigenic [43]. Large amounts of studies confirmed that smectite could be formed rapidly from the intermediate-basic volcanic rocks when involved in sufficient water [12,43,45].

The Ontong Java Plateau was formed from the eruption of mantle basaltic magma during Cretaceous and its basement is the intermediate-basic volcanic rocks. Moreover, Banerjee et al. [46] found the clear low-temperature alteration of smectite by analyzing basement samples collected from the Ontong Java Plateau during the Ocean Drilling Program (ODP) Leg 192. Therefore, prior to interpreting the paleoenvironmental change using clay mineralogy, it is critical to determine the formation of smectite at Core KX21-2.

In general, multiple coupled analyses could effectively determine the formation of smectite, such as provenance analysis, morphology of mineral grains, mineral crystallinity, geochemical compositions, REE (rare Earth elements) patterns, mineral assemblage characters, etc. [47]. In this study, first of all, the clay mineral assemblages at Core KX21-2 (with the predominance of smectite) are in accordance with the geological settings of adjacent land masses (i.e. the lithology of New Guinea consists mainly of the intermediate-basic volcanic rocks and sedimentary rocks, Figure 1), corresponds well to the provenance analysis of clay minerals (see details in section 4.2). Secondly, the photomicrography of randomly selected samples shows that clay mineral particles are not found with any authigenic character (e.g. the honey-comb pattern). Along with the EDS analysis, Fe-, Mg-, and Na-smectite grains [12] are observed in bedded and laminated accumulations (Figure 4), demonstrating that the clay minerals are mainly terrigenous clastics and their post-deposition diagenesis could be negligible. Thirdly, considering homogeneity, rapidity, and abundance characters of authigenic clay minerals [43], a low proportion (~20%) of clay-sized minerals at Core

KX21-2 can result from its geographical location, instead of the low-temperature alteration of volcanic materials in the marine environment. Most importantly, variations in the smectite content are well correlated to those in the feldspar/quartz ratio and the smectite crystallinity (Figure 3), and furthermore the spectral analyses of variations in the smectite content and the feldspar/quartz ratio show a similar result (Figure 5). These factors suggest that the formation of smectite is directly related to the weathering and erosion. Therefore, it can be concluded that the smectite at Core KX21-2 is the terrigenous detrital origin and that late Quaternary sediments on the Ontong Java Plateau does not suffer from the diagenesis, unlike the basement of the Ontong Java Plateau [46].

4.2 Provenance of clay minerals

The sedimentological study on ODP Leg 130 sediments suggested that the Ontong Java Plateau received aeolian deposits from many provenances, mainly including aeolian dusts from Asia and nearby land masses [48]. Rea [49] proposed that the Asian dust could be transported by the west trades and then by the northeast trades in different elevations, respectively, and finally be settled in the equatorial ocean due to the meridional migration of the ITCZ. By analyzing biotic proxies like the foraminifer assemblages at ODP Site 807, Zhang et al. [50] found that the increase of surface productivity in the central WPWP was not related to other ways of the nutrients supply, and then deduced the effect of the influx of Asian dust. Furthermore, Patterson et al. [51] and Winckler et al. [52] reconstructed the history of aeolian dust input deposition at ODP Site 806 using the flux of ^{4}He and ^{232}Th, respectively. The results suggested that the Asian dust is an important source for sediments on the Ontong Java Plateau and the dust input responds to the climate change in glacial cycles. By comparing the iron flux of the Xifeng Loess with the ^{232}Thflux at ODP Site 806, Guo et al. [53] presented their good correlation to further support the aeolian dust origin. In addition, geochemical studies in the equatorial Pacific also revealed that the aeolian dust accounts for certain proportions [54–56].

However, neither the remote Asian dust nor the nearby Australian dust is qualified to be the major source of clay minerals on the Ontong Java Plateau. Clay mineral assemblage of the Quaternary loess is mainly composed of illite, with few smectite (<10%) [57,58]. As a consequence, the Asian dust comprising mostly the loess could not be the main source of clay minerals at Core KX21-2. The Australian dust is the other possibility, but both geological records and numerical models manifested that the Australian dust hardly reaches the central part of WPWP due to its northwest-southeast transport pathway [59]. Moreover, previous studies suggested that smectite and chlorite are rich in Fe^{3+} and Fe^{2+}, respectively. Changes in the Fe content are similar

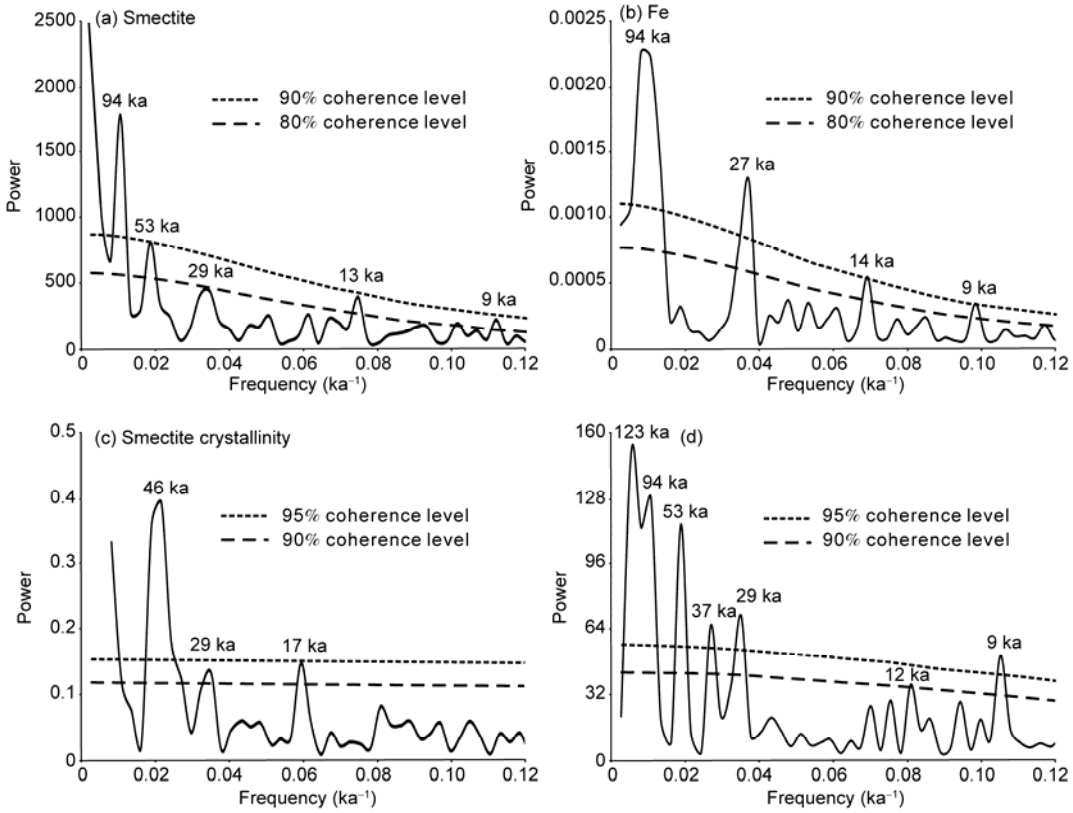

Figure 5 Spectral analyses of smectite content, Fe content, feldspar/quartz ratio, and smectite crystallinity at Core KX21-2.

to those in the smectite content but contrary to the chlorite content, presenting higher frequency oscillations (Figure 2) [12,43]. These reveal that the iron is primarily carried by smectite, and that the Fe content can be used to indicate the changes in the smectite content. Observations and models illustrated that the impact of dust deposit on the western equatorial Pacific is limited, with low flux of iron (<10 mg m^{-2} a^{-1}) [60,61] and no seasonal change [62], further confirming that the major source of smectite is other provenance, instead of the aeolian dust.

By scrutinizing all the evidence for aeolian dust, some problems were found. First of all, Krissek and Janecek [48] presented the stably high content of smectite since 33 Ma ago, and agreed that its origin is irrelevant to the Asian dust. Considering that the Ontong Java Plateau is far from land masses and the fluvial inputs should be limited, they ascribed the origin of smectite to the unknown adjacent dust, and this is apparently unwarranted. To the contrary, according to their studies, the increase of smectite content during 3–7 Ma ago [48] could be temporally related to the active tectonic movements over New Guinea, resulting in the enrichment of terrigenous materials and rearrangement of oceanic currents [63]. Secondly, the dust fluxes of the equatorial Pacific estimated by different methods vary widely, and tend to be an order of magnitude higher than the model results [52]. These differences can be attributed to the calculation of mass accumulation rate: the ^{230}Th normalization, as the foundation of various studies of dust flux [52,54,55], is now being questioned [64,65] and still requires more constraints from modern observations. Thirdly, if conceding that the aeolian dust is the major terrigenous component in the equatorial Pacific, owing to the increased washout by precipitation, a maximum in terrigenous flux would be expected to occur under the location of ITCZ (3°–7°N nowadays), and should vary in response to the shift of the ITCZ. Nevertheless, that is not yet being verified [55]. Additionally, since the terrigenous sources in the equatorial Pacific are highly sensitive to the change of latitudes, it should be taken into account the apparent regional effects [56].

On the basis of the above discussions, we argue that the terrigenous materials on the Ontong Java Plateau are mainly provided by the river detrital inputs of New Guinea. This view has been supported by a variety of studies such as the Source-to-Sink (S2S) Project within the MARGINS Program, the Joint Global Ocean Flux Study (JGOFS), the Tropical River Ocean Processes in Coastal Settings (TROPICS), etc. Below, we briefly show evidence from three respects: river inputs, S2S processes, and current configuration.

Firstly, Milliman and Syvitski [5] broke the traditional cognition: until then, the importance of the small mountainous rivers on terrigenous contribution had always been underestimated, especially considering that these rivers tend to develop along with the active margin shelf. Heavy rainfall, active tectonic activities, relatively erodible rocks, as well as characteristics of river drainage basins including high topographic relief, short transport distance, and small catchment area, can create extremely strong mechanical erosion at the island of New Guinea. For instance, the Sepik River contributes about 1×10^8 t a^{-1} fluvial sediments with a drainage basin area of only 77700 km^2, and its sediment yields based on measurements in the middle and lower reaches exceeds 1000 t km^{-2} a^{-1} [11,22].

Secondly, it was previously believed that fluvial materials tend to deposit near estuaries, rather than being transported into the deep sea and this was confirmed by studies on the distribution of clay minerals in the oceans [41–43]. However, with the better understanding of the S2S process, it is aware of that this view is not completely true. The northern and southern New Guinea have the contrasting styles of sediment accumulation. When the sea level is high, most inputs of the Fly River in the southern New Guinea deposit on the broad shelf; only few materials could be carried to the deep sea by surface currents when the northwest monsoon prevails, and then incorporates in the subsurface currents [6,7,11,24]. In contrast, on the active continental margin, river inputs can directly bypass the slope via high-density turbidity currents and such like ways induced by sediment gravity, and even transport for a long distance within the oceanic currents, regardless of sea level change. The Sepik River in the northern New Guinea is a case in point [6,7,10,11,23,24].

Thirdly, based on the oceanic current configuration in the WPWP [25–29], a variety of studies including neodymium [17] and osmium isotopes [66], distributions of iron, aluminum and manganese [7,18,67,68], REE compositions [16], simulations [69], and sediment trap records [70] indicate that the terrigenous materials from the river inputs of New Guinea could be transported by currents to the Ontong Java Plateau (Figure 1). And this oceanic current system has been stably existed since early Pliocene [56,63].

In combination with our study results, Core KX15-2 is situated both in the estuary of the Sepik River and also at the pathway of NGCUC and its cop-top sample contains as high as 90% of smectite, which can be approximately regarded as the clay mineral assemblage of river materials in New Guinea. Core KX12-1 and Core KX13-1 are far away from the estuaries, and the smectite contents of their core-top samples are 61% and 65%, respectively, lower than that at Core KX15-2 and Core KX21-2. This could be ascribed to the effect of differential settling process. Therein, the phenomenon that the smectite content of core-top sample at Core KX12-1 is even lower than that at Core KX13-1 is probably because the location of Core KX12-1 is farther from the coastline and the pathway of NGCUC.

To sum up, we believe that the clay minerals with a majority of smectite at Core KX21-2 derive mainly from the rivers of New Guinea. Asian dust could also provide a small portion of clay minerals that contain few smectite. Due to the differences in clay mineral assemblages between the

river inputs of New Guinea and the Asian dust, the clay minerals especially the smectite content and its synchronous Fe content can be used as proxies to indicate the terrigenous inputs to the Ontong Java Plateau.

The time series of variation in clay minerals at Core KX21-2 is dominated by the river inputs of New Guinea. Regardless of the sea level change, the fluvial materials from the northern New Guinea (e.g. Sepik River) can travel across the narrow shelf, then be transported by the subsurface currents (mainly NGCUC) crossing the Bismarck Sea and the Solomon Sea, and ultimately merge into the EUC and deposit on the Ontong Java Plateau. In contrast, owing to the difference in the S2S process, the sediment yield in the southern New Guinea is smaller and more susceptible to the sea level change and monsoon climate. During the interglacials, the coastline of the southern New Guinea is analogous with today's, most fluvial materials deposit on the broad shelf, and only few could be carried southwards via surface currents driven by the northwest monsoon, then incorporated in the subsurface currents (GBRUC), and finally deposited in the western equatorial Pacific. In the glacials, the coastline shifted to about 100 m depth contour (Figure 1), much of the fluvial inputs can be channeled to deep sea. In particular during the deglacials, the rapid sea level rise could probably bring a huge amount of sediments deposited on the southern broad shelf into the deep sea, causing the sharp rises in smectite and Fe content (Figure 2). Therefore, although the clay mineral assemblages provided from the southern and northern New Guinea are similar, the fluctuations of sea level coupled with the contrasting styles of the S2S process over New Guinea have resulted in the glacial-interglacial cycle of clay mineral assemblages at Core KX21-2.

4.3 Migration of ITCZ

According to the provenance analysis, the variations in clay mineral assemblages at Core KX21-2 reflect the terrigenous supply from the source regions, and the glacial-interglacial cyclicity is closely related to the sea level change. The spectral analysis shows a strong 94 ka eccentricity period, and the smectite and Fe content also have 29, 13 and 9, and 27, 14 and 9 ka periods, respectively (Figure 5), which are in accordance with the astronomical precessional periods or semi-precessional periods [71]. Hence, the variations in clay minerals present characteristics of tropical processes. The question is how these characteristics are expressed?

By synthesizing a variety of paleo-monsoon records from the subtropical-tropical regions in the Northern and Southern Hemispheres, Wang et al. [72] revealed an explicit anti-phase relationship between inter-hemispheric precipitation both on the orbital and millennial timescales, with increased monsoon rainfall in one hemisphere while decreased in the other. This inter-hemispheric "see-saw" pattern in hydrological cycles is attributed to the displacement in the mean position of the ITCZ accompanied by the meridional asymmetry in the Hadley circulation.

On the millennial scale, it is generally acknowledged that the inter-hemispheric "see-saw" pattern in monsoon rainfall is applicable to the Australian-Asian monsoon system. For example, the arid condition occurred during the D/O events in northeastern Australia, while the humid condition happened in the Heinrich events, coinciding with the meridional migration of the ITCZ [73,74]. On the orbital scale, this anti-phase relationship is also explicitly expressed by monsoon records from North and South Africa [75,76], as well as the marine [2] and stalagmite records [3,77] from South America. Nevertheless, given its complexity of the Australian-Asian monsoon system, the forcing mechanism on the orbital scale is still not fully understood.

Both simulation results [78–81] and geological archives [20,82,83] illustrate that the intensity of Australian summer monsoon is directly controlled by the summer insolation in the Southern Hemisphere. On the other hand, during winters of the Northern Hemisphere, the Siberian High system would drive the strong cross-equatorial flow [84,85], thereby exerting a significant influence on the precipitation in the Australian-Asian monsoon system through the insolation-related East Asian monsoon [86–89]. In brief, we believe that the monsoon is essentially expression of the seasonal migration of the ITCZ [1]. As the most important rainfall zone, the shift of the ITCZ is closely related to the change of atmospheric heat exchange on any time scale [90], and is controlled by insolation and land-sea distribution [79,80]. Therefore, the migration of the ITCZ not only presents typical processional periods [91], but also exhibits clear regional characteristics [83].

Variations in the smectite content at Core KX21-2 are well correlated positively with those in the feldspar/quartz ratio and are inversely with those in the smectite crystallinity (Figure 3), demonstrating that the higher smectite content indicate the stronger mechanical erosion intensity instead of weaker chemical weathering intensity, and *vice versa*. The clay mineralogy of core-top samples also supports this viewpoint: the more smectite content, the higher feldspar/quartz ratio and the better smectite crystallinity (Table 1). Therefore, despite the hot and humid climatic conditions throughout the year in New Guinea, some regional environmental factors including active tectonic setting, strong precipitation, and mountainous rivers (high topographic relief, small catchment area, and short transport distance) are responsible for the limited time that allows the chemical weathering well develops, resulting in the predominance of smectite (this is not the final weathering product). Therefore, smectite here should indicate the intensity of mechanical erosion, responding to the river runoff and precipitation. This process is highly analogous to the situation of illite and chlorite provided by rivers in Taiwan [92].

Modern climatic records show that the precipitation distribution of New Guinea is affected by the shift of the

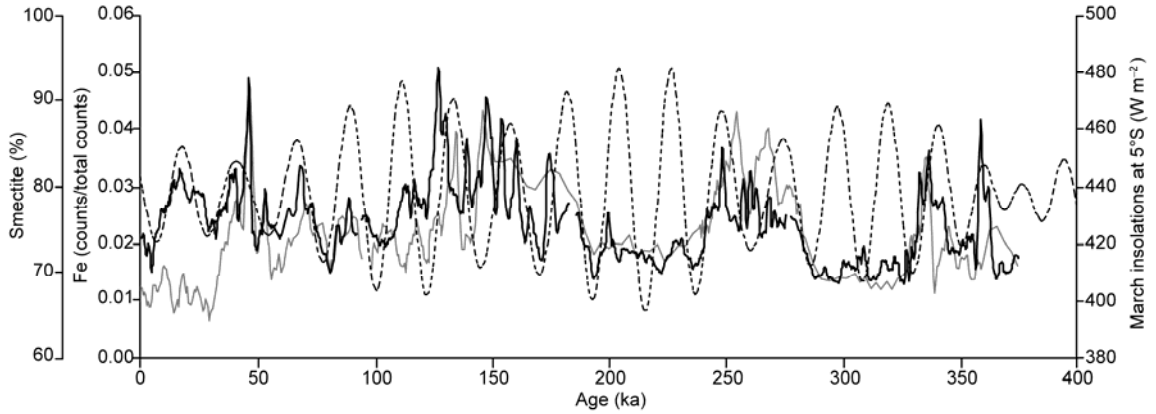

Figure 6 Comparisons between smectite and Fe contents at Core KX21-2 and the mean insolation of March at 5°S. The smectite and Fe contents were smoothed by a five-point moving average. Insolation data are from [93].

ITCZ, presenting obvious seasonal change. During the winter of the Northern Hemisphere, the ITCZ moves southwards, and the northwest monsoon (Australian summer monsoon) brings a huge amount of water vapor, resulting in increased rainfall; while during the summer, the ITCZ shifts northwards, and the Australian continent-originated southeast monsoon (Australian winter monsoon) prevails, resulting in reduced precipitation. A good correlation exists between the smectite and Fe contents with the mean insolation of March (the Sun is on the equinox) at 5°S (position of New Guinea) (Figure 6). Therefore, we proposed that variations in the smectite content at Core KX21-2 are directly related to the precipitation distribution in New Guinea, reflecting the meridional migration of the ITCZ on the orbital scale. Besides, the spectral analysis on the smectite crystallinity also demonstrates clear precessional and semi-precessional periods, without the signal of sea level change (Figure 5), implying that the hydrolysis is closely correlated to the ITCZ-controlled precipitation.

In summary, besides the effect from the sea level change, variations in the smectite content at the precessional periods indicate the intensity of mechanical erosion in the source region, the island of New Guinea, responding to the river runoff and precipitation. The smectite content then further reflects the shift of the ITCZ on the orbital scale. When the summer insolation in the Southern Hemisphere is high, the mean position of ITCZ moves southwards and brings heavy rainfall, and *vice versa*.

5 Conclusions

Through the provenance analysis of clay minerals and its temporal variations over the past 370 ka during late Quaternary from Core KX21-2 in the WPWP, combined with elemental XRF scanning data and regional setting study, we obtain the following conclusions: (1) The clay mineral assemblages at Core KX21-2 are composed dominantly of smectite (62%–91%), with minor chlorite (4%–21%), illite (4%–12%), and kaolinite (2%–10%). Variations in the clay minerals show the prominent glacial-interglacial cyclicity, with higher smectite contents during interglacials than glacials. Three other minerals share a similar variation pattern, but mirroring to that of smectite. (2) The smectite-dominated clay minerals are terrigenous detritals and most of them derive from the river inputs of New Guinea. The Asian dust could provide a portion of clay minerals but much less than New Guinea. (3) The glacial-interglacial cyclicity of clay mineral assemblages is in coherence with the sea level change. During the low sea level periods, the river inputs could more easily bypass the narrow shelf off the island of New Guinea, then travel within the subsurface currents, and ultimately deposit on the central part of the WPWP. (4) The precessional periods of the smectite content present the intensity of mechanical erosion in its provenance of New Guinea, responding to the river runoff and precipitation, and furthermore reflecting the meridional migration of the ITCZ on the orbital scale.

All the samples used in this study were provided by cruise KX08-973, which is sponsored by the National Basic Research Program of China. We thank the crew and scientists aboard the R/V Kexue-1. Zhao Yulong, Dang Haowen, and He Ziding are thankful for their helpful discussions, and Wang Hao is thankful for his assistance in figure preparations. We are appreciative of three anonymous reviewers for their critical and constructive comments that are considerably helpful to improve this paper. This work was supported by the National Natural Science Foundation of China (40925008 and 91128206) and the National Basic Research Program of China (2007CB815906).

1 Wang P. Global monsoon in a geological perspective. Chin Sci Bull, 2009, 54: 1113–1136
2 Haug G H, Hughen K A, Sigman D M, et al. Southward migration of the intertropical convergence zone through the Holocene. Science, 2001, 293: 1304–1308
3 Wang X F, Auler A S, Edwards R L, et al. Wet periods in northeastern Brazil over the past 210 ka linked to distant climate anomalies. Nature, 2004, 432: 740–743
4 Yancheva G N, Nowaczyk N R, Mingram J, et al. Influence of the intertropical convergence zone on the East Asian monsoon. Nature,

2007, 445: 74–77
5 Milliman J D, Syvitski J M. Geomorphic/tectonic control of sediment discharge to the ocean: The Importance of small mountainous Rivers. J Geol, 1992, 100: 525–544
6 Milliman J D. Sediment discharge to the ocean from small mountainous rivers: The New Guinea example. Geo-Mar Lett, 1995, 15: 127–133
7 Milliman J D, Farnsworth K L, Albertin A S. Flux and fate of fluvial sediments leaving large islands in the East Indies. J Sea Res, 1999, 41: 97–107
8 Lea D W, Pak D K, Spero H J. Climate impact of late quaternary equatorial Pacific sea surface temperature variations. Science, 2000, 289: 1719–1724
9 Rosenthal Y, Oppo D W, Linsley B K. The amplitude and phasing of climate change during the last deglaciation in the Sulu Sea, western equatorial Pacific. Geophys Res Lett, 2003, 30: 8
10 Kineke G C, Woolfe K J, Kuehl S A, et al. Sediment export from the Sepik River, Papua New Guinea: Evidence for a divergent sediment plume. Cont Shelf Res, 2000, 20: 2239–2266
11 Walsh J P, Nittrouer C A. Contrasting styles of off-shelf sediment accumulation in New Guinea. Mar Geol, 2003, 196: 105–125
12 Chamley H. Clay Sedimentology. Berlin: Springer, 1989. 1–623
13 Colin C H, Turpin L, Bertaux J, et al. Erosional history of the Himalayan and Burman ranges during the last two glacial-interglacial cycles. Earth Planet Sci Lett, 1999, 171: 647–660
14 Gingele F X, De Deckker P, Hillenbrand C D. Clay mineral distribution in surface sediments between Indonesia and NW Australia—source and transport by ocean currents. Mar Geol, 2001, 179: 135–146
15 Liu Z F, Trentesaux A, Clemens S C, et al. Clay mineral assemblages in the northern South China Sea: Implications for East Asian monsoon evolution over the past 2 million years. Mar Geol, 2003, 201: 133–146
16 Sholkovitz E R, Elderfield H, Szymczak R, et al. Island weathering: River sources of rare earth elements to the Western Pacific Ocean. Mar Chem, 1999, 68: 39–57
17 Lacan F, Jeandel C. Tracing Papua New Guinea imprint on the central Equatorial Pacific Ocean using neodymium isotopic compositions and Rare Earth Element patterns. Earth Planet Sci Lett, 2001, 186: 497–512
18 Mackey D J, O'Sullivan J E, Watson R J. Iron in the western Pacific: A riverine or hydrothermal source for iron in the Equatorial Undercurrent? Deep-Sea Res Pt I, 2002, 49: 877–893
19 van der Kaars S, Wang X, Kershaw P, et al. A Late Quaternary palaeoecological record from the Banda Sea, Indonesia: Patterns of vegetation, climate and biomass burning in Indonesia and northern Australia. Palaeogeogr Palaeoclimatol Palaeoecol, 2000, 155: 135–153
20 Kershaw A P, van der Kaars S, Moss P T. Late Quaternary Milankovitch-scale climatic change and variability and its impact on monsoonal Australasia. Mar Geol, 2003, 201: 81–95
21 Commission for the Geological Map of the World, 1975. Geological World Atlas, scale 1:10000000. UN Educ. Sci Cult Org, Paris
22 Chappell J. Contrasting Holocene sedimentary geologies of lower Daly River, northern Australia, and lower Sepik-Ramu, Papua New Guinea. Sediment Geol, 1993, 83: 339–358
23 Kuehl S A, Brunskill G J, Burns K, et al. Nature of sediment dispersal off the Sepik River, Papua New Guinea: Preliminary sediment budget and implications for margin processes. Cont Shelf Res, 2004, 24: 2417–2429
24 Brunskill G. New Guinea and its coastal seas, a testable model of wettropical coastal processes: An introduction to Project TROPICS. Cont Shelf Res, 2004, 24: 2273–2295
25 Lindstrom E, Lukas R, Fine R, et al. The Westem Equatorial Pacific Ocean circulation study. Nature, 1987, 330: 533–537
26 Tsuchiya M, Lukas R, Fine R, et al. Source waters of the Pacific Equatorial Undercurrent. Prog Oceanogr, 1989, 23: 101–147
27 Butt J, Lindstrom E. Currents off the east-coast of New-Ireland, Papua-New-Guinea, and their relevance to regional undercurrents in the Western Equatorial Pacific-Ocean. J Geophys Res-Oceans, 1994, 99: 12503–12514
28 Fine R, Lukas R, Bingham F, et al. The Western Equatorial Pacific —A Water Mass Crossroads. J Geophys Res-Oceans, 1994, 99: 25063– 25080
29 Cresswell G R. Coastal currents of northern Papua New Guinea, and the Sepik River outflow. Mar Freshwater Res, 2000, 51: 553–564
30 Zhou C, Jin H, Jian Z. Variations of the late quaternary Paleoproductivity in the western equatorial Pacific: Evidence from the elemental ratios (in Chinese). Quat Sci, 2011, 31: 1–9
31 Holtzapffel T. Les minéraux argileux: Préparation, analyse diffractométrique et determination. Soc Géol Nord Publ 12, 1985. 1–136
32 Liu Z, Colin C, Trentesaux A, et al. Erosional history of the eastern Tibetan Plateau over the past 190 ka: Clay mineralogical and geochemical investigations from the southwestern South China Sea. Mar Geol, 2004, 209: 1–18
33 Petschick R. MacDiff 4.2.2. http://servermac.geologie.un-frankfurt.de/Rainer.html, 2000
34 Liu Z, Colin C, Li X, et al. Clay mineral distribution in surface sediments of the northeastern South China Sea and surrounding fluvial drainage basins: Source and transport. Mar Geol, 2010, 277: 48–60
35 Petschick R, Kuhn G, Gingele F. Clay mineral distribution in surface sediments of the South Atlantic: Sources, transport, and relation to oceanography. Mar Geol, 1996, 130: 203–229
36 Liu Z F, Zhao Y L, Colin C, et al. Chemical weathering in Luzon, Philippines from clay mineralogy and major-element geochemistry of river sediments. Appl Geochem, 2009, 24: 2195–2205
37 Kuhn G, Diekmann B. Late Quaternary variability of ocean circulation in the southeastern South Atlantic inferred from the terrigenous sediment record of a drift deposit in the southern Cape Basin (ODP Site 1089). Palaeogeogr Palaeoclimatol Palaeoecol, 2002, 182: 287–303
38 Diekmann B, Kuhn G. Sedimentary record of the mid-Pleistocene climate transition in the southeastern South Atlantic (ODP Site 1090). Palaeogeogr Palaeoclimatol Palaeoecol, 2002, 182: 241–258
39 Revel M, Ducassou E, Grousset F, et al. 100000 years of African monsoon variability recorded in sediments of the Nile margin. Quat Sci Rev, 2010, 29: 1342–1362
40 Schulz M, Mudelsee M. REDFIT: Estimating red-noise spectra directly from unevenly spaced paleoclimatic time series. Comput Geosci, 2002, 28: 421–426
41 Biscaye P E. Mineralogy and sedimentation of recent deep-sea clay in the Atlantic Ocean and adjacent seas and oceans. Geol Soc Am Bull, 1965, 76: 803–832
42 Griffin J J, Windom H, Goldberg E D. The distribution of clay minerals in the world ocean. Deep Sea Res Oceanogr Abs, 1968, 15: 433–459
43 Fagel N. Clay minerals, deep circulation and climate. In: Hillaire-Marcel C, De Vernal A, eds. Proxies in Late Cenozoic Paleoceanography. Paris: Elservier, 2007. 139–184
44 Grinffin G M. Regional clay mineral facies-products of weathering intensity and current distribution in the northeastern Gulf of Mexico. Geol Soc Am Bull, 1962, 73: 737–768
45 Thiry M. Palaeoclimatic interpretation of clay minerals in marine deposits: an outlook from the continental origin. Earth-Sci Rev, 2000, 49: 201–221
46 Banerjee N, Honnorez J, Muehlenbachs K. Low-temperature alteration of submarine basalts from the Ontong Java Plateau. In: Fitton J G, Mahoney J J, Wallace P J, eds. Origin and Evolution of the Ontong Java Plateau. London: Geological Society, 2005. 259–273
47 Chen T, Wang H, Zhang Z, et al. Clay minerals as indicators of paleoclimate (in Chinese). Acta Petrol Mineral, 2003, 22: 416–420
48 Krissek L A, Janecek T R. Eolian deposition on the Ontong Java Plateau since the Oligocene: Unmixing a record of multiple dust sources. In: Berger W H, Kroenke L W, Mayer L A, et al., eds. Proceedings of the Ocean Drilling Program, Scientific Results, 1993, 130: 471–490
49 Rea D K. The paleoclimatic record provided by eolian deposition in the deep-sea—the geologic history of wind. Rev Geophys, 1994, 32: 159–195
50 Zhang J Y, Wang P X, Li Q Y, et al. Western equatorial Pacific

productivity and carbonate dissolution over the last 550 ka: Foraminiferal and nannofossil evidence from ODP Hole 807A. Mar Micropaleontol, 2007, 64: 121–140
51 Patterson D B, Farley K A, Norman M D. He-4 as a tracer of continental dust: A 1.9 million year record of aeolian flux to the west equatorial Pacific Ocean. Geochim Cosmochim Acta, 1999, 63: 615–625
52 Winckler G, Anderson R F, Fleisher M Q, et al. Covariant glacial-interglacial dust fluxes in the equatorial Pacific and Antarctica. Science, 2008, 320: 93–96
53 Guo Z T, Berger A, Yin Q Z, et al. Strong asymmetry of hemispheric climates during MIS-13 inferred from correlating China loess and Antarctica ice records. Clim Past, 2009, 5: 21–31
54 Anderson R F, Fleisher M Q, Lao Y. Glacial-interglacial variability in the delivery of dust to the central equatorial Pacific Ocean. Earth Planet Sci Lett, 2006, 242: 406–414
55 McGee D, Marcantonio F, Lynch-Stieglitz J. Deglacial changes in dust flux in the eastern equatorial Pacific. Earth Planet Sci Lett, 2007, 257: 215–230
56 Ziegler C L, Murray R W, Plank T, et al. Sources of Fe to the equatorial Pacific Ocean from the Holocene to Miocene. Earth Planet Sci Lett, 2008, 270: 258–270
57 Kalm V E, Rutter N W, Rokosh C D. Clay minerals and their paleoenvironmental interpretation in the Baoji loess section, Southern Loess Plateau, China. Catena, 1996, 27: 49–61
58 Gylesjo S, Arnold E. Clay mineralogy of a red clay-loess sequence from Lingtai, the Chinese Loess Plateau. Glob Planet Change, 2006, 51: 181–194
59 Mackie D S, Boyd P W, McTainsh G H, et al. Biogeochemistry of iron in Australian dust: From eolian uplift to marine uptake. Geochem Geophys Geosys, 2008, 9: Q03Q08
60 Gao Y, Fan S M, Sarmiento J L. Aeolian iron input to the ocean through precipitation scavenging: A modeling perspective and its implication for natural iron fertilization in the ocean. J Geophys Res-Atmos, 2003, 108: D7
61 Duce R A, Tindale N W. Atmospheric transport of iron and its deposition in the ocean. Limnol Oceanogr, 1991, 36: 1715–1726
62 Gao Y, Kaufman Y J, Tanre D, et al. Seasonal distributions of aeolian iron fluxes to the global ocean. Geophys Res Lett, 2001, 28: 29–32
63 Wells M L, Vallis G K, Silver E A. Tectonic processes in Papua New Guinea and past productivity in the eastern equatorial Pacific Ocean. Nature, 1999, 398: 601–604
64 Lyle M, Pisias N, Paytan A, et al. Do geochemical estimates of sediment focusing pass the sediment test in the equatorial Pacific? Paleoceanography, 2005, 20: Pa1005
65 Lyle M, Pisias N, Paytan A, et al. Reply to comment by R. Francois et al. on "Do geochemical estimates of sediment focusing pass the sediment test in the equatorial Pacific": Further explorations of ^{230}Th normalization. Paleoceanography, 2007, 22: Pa1217
66 Martin C E, Peucker-Ehrenbrink B, Brunskill G J, et al. Sources and sinks of unradiogenic osmium runoff from Papua New Guinea. Earth Planet Sci Lett, 2000, 183: 261–274
67 Coale K H, Fitzwater S E, Gordon R M, et al. Control of community growth and export production by upwelled iron in the equatorial Pacific Ocean. Nature, 1996, 379: 621–624
68 Gordon R M, Coale K H, Johnson K S. Iron distributions in the equatorial Pacific: Implications for new production. Limnol Oceanogr, 1997, 42: 419–431
69 Ryan J P, Ueki I, Chao Y, et al. Western Pacific modulation of large phytoplankton blooms in the central and eastern equatorial Pacific. J Geophys Res-Biogeol, 2006, 111: G02013
70 Kawahata H. Fluctuations in the ocean environment within the western Pacific warm pool during late Pleistocene. Paleoceanography, 1999, 14: 639–652
71 Ruddiman W F. Earth's Climate: Past and Future. New York: W. H. Freeman and Company. 2001. 1–465
72 Wang X F, Auler A S, Edwards R L, et al. Interhemispheric antiphasing of rainfall during the last glacial period. Quat Sci Rev, 2006, 25: 3391–3403
73 Turney C M, Kershaw A P, Clemens S C, et al. Millennial and orbital variations of El Nino/Southern Oscillation and high-latitude climate in the last glacial period. Nature, 2004, 428: 306–310
74 Muller J, Kylander M, Wust R, et al. Possible evidence for wet Heinrich phases in tropical NE Australia: The Lynch's Crater deposit. Quatern Sci Rev, 2008, 27: 468–475
75 Partridge T C. Cainozoic environmental change in southern Africa, with special emphasis on the last 200000 years. Prog Phys Geogr, 1997, 21: 3–22
76 Partridge T C, Demenocal P B, Lorentz S A, et al. Orbital forcing of climate over South Africa: A 200000-year rainfall record from the Pretoria Saltpan. Quat Sci Rev, 1997, 16: 1125–1133
77 Cruz F W, Burns S J, Karmann I, et al. Insolation-driven changes in atmospheric circulation over the past 116000 years in subtropical Brazil. Nature, 2005, 434: 63–66
78 Liu Z, Brady E, Lynch-Stieglitz J. Global ocean response to orbital forcing in the Holocene. Paleoceanography, 2003, 18: 1041
79 Wyrwoll K H, Valdes P. Insolation forcing of the Australian monsoon as controls of Pleistocene mega-lake events. Geophys Res Lett, 2003, 30: 2279
80 Wyrwoll K H, Liu Z Y S, Chen G, et al. Sensitivity of the Australian summer monsoon to tilt and precession forcing. Quat Sci Rev, 2007, 26: 3043–3057
81 Kutzbach J E, Liu X D, Liu Z Y, et al. Simulation of the evolutionary response of global summer monsoons to orbital forcing over the past 280000 years. Clim Dyn, 2008, 30: 567–579
82 Bowler J M, Wyrwoll K H, Lu Y C. Variations of the northwest Australian summer monsoon over the last 300000 years: The paleohydrological record of the Gregory (Mulan) Lakes System. Quat Int, 2001, 83-85: 63–80
83 Holbourn A, Kuhnt W, Kawamura H, et al. Orbitally paced paleoproductivity variations in the Timor Sea and Indonesian Throughflow variability during the last 460 ka. Paleoceanography, 2005, 20: Pa3002
84 Liu T S, Ding Z L. Chinese loess and the paleomonsoon. Annu Rev Earth Planet Sci, 1998, 26: 111–145
85 An Z S. The history and variability of the East Asian paleomonsoon climate. Quat Sci Rev, 2000, 19: 171–187
86 Magee J W, Miller G H, Spooner N A, et al. Continuous 150 ky monsoon record from Lake Eyre, Australia: Insolation-forcing implications and unexpected Holocene failure. Geology, 2004, 32: 885–888
87 Miller G, Mangan J, Pollard D, et al. Sensitivity of the Australian Monsoon to insolation and vegetation: Implications for human impact on continental moisture balance. Geology, 2005, 33: 65–68
88 Luckge A, Mohtadi M, Ruhlemann C, et al. Monsoon versus ocean circulation controls on paleoenvironmental conditions off southern Sumatra during the past 300000 years. Paleoceanography, 2009, 24: PA1208
89 Mohtadi M, Luckge A, Steinke S, et al. Late Pleistocene surface and thermocline conditions of the eastern tropical Indian Ocean. Quat Sci Rev, 2010, 29: 887–896
90 Broccoli A J, Dahl K A, Stouffer R J. Response of the ITCZ to Northern Hemisphere cooling. Geophys Res Lett, 2006, 33: L01702
91 Prell W L, Kutzbach J E. Sensitivity of the Indian monsoon to forcing parameters and implications for its evolution. Nature, 1992, 360: 647–652
92 Liu Z, Tuo S, Colin C, et al. Detrital fine-grained sediment contribution from Taiwan to the northern South China Sea and its relation to regional ocean circulation. Mar Geol, 2008, 255: 149–155
93 Laskar J, Robutel P, Joutel F, et al. A long-term numerical solution for the insolation quantities of the Earth. A&A, 2004, 428: 261–285